Accepted Manuscript

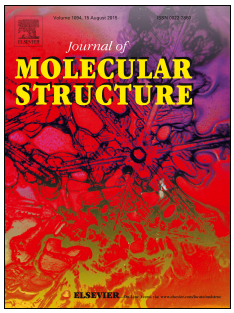

Silver(I)-pyridinyl Schiff base complexes: Synthesis, characterization and antimicrobial studies

Eric M. Njogu, Bernard Omondi, Vincent O. Nyamori

PII: S0022-2860(17)30092-3

DOI: 10.1016/j.molstruc.2017.01.061

Reference: MOLSTR 23366

To appear in: *Journal of Molecular Structure*

Received Date: 11 August 2016

Revised Date: 18 January 2017

Accepted Date: 20 January 2017

Please cite this article as: E.M. Njogu, B. Omondi, V.O. Nyamori, Silver(I)-pyridinyl Schiff base complexes: Synthesis, characterization and antimicrobial studies, *Journal of Molecular Structure* (2017), doi: 10.1016/j.molstruc.2017.01.061.

Silver(I)-pyridinyl Schiff base complexes: Synthesis, characterization and antimicrobial studies

Eric M. Njogu, Bernard Omondi and Vincent O. Nyamori

School of Chemistry and Physics, University of KwaZulu-Natal, South Africa

Private bag X54001, Durban, 4000

Email: bjumberic2002@gmail.com; owaga@ukzn.ac.za; nyamori@ukzn.ac.za

Graphical abstract

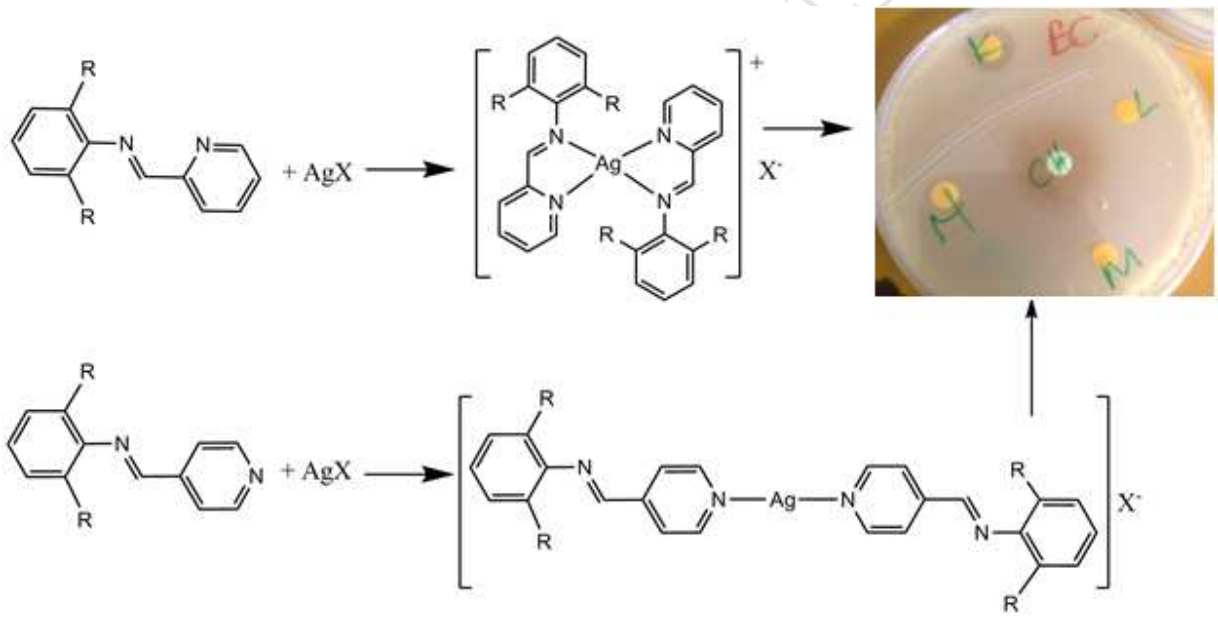

Scheme showing the synthesis of silver(I)-pyridinyl complexes and the antimicrobial screening

Silver(I)-pyridinyl Schiff base complexes: Synthesis, characterization and antimicrobial studies

Eric M. Njogu, Bernard Omondi and Vincent O. Nyamori

School of Chemistry and Physics, University of KwaZulu-Natal, South Africa

Private bag X54001, Durban, 4000

Email: bjumberic2002@gmail.com; owaga@ukzn.ac.za; nyamori@ukzn.ac.za

Abstract

Fifteen new silver(I)-pyridinyl complexes of the general formula $[AgL_2]X$, where X = ClO_4^-, OTf or NO_3^-, were synthesised by reacting (*E*)-*N*-(pyridinylmethylene)aniline ligands and the respective silver(I) salts namely $AgClO_4$, AgOTf, or $AgNO_3$. The ligands were obtained by neat grinding of 2- or 4-pyridincarboaxaldehyde together with aniline, 2,6-dimethylaniline or 2,6-diisopropylaniline. The obtained (*E*)-*N*-(pyridinylmethylene)aniline ligands were further reacted with respective silver(I) salts in a 2:1 ratio in anhydrous ethanol at room temperature under inert atmosphere using the Schlenk techniques. Chemical structures of complexes were identified by nuclear magnetic resonance, electrospray ionization mass spectrometry, elemental analysis, infrared spectroscopy and some by single-crystal X-ray diffraction analysis. Reactions involving the 2-pyridinyl derivatives resulted in cationic complexes in which two ligands chelate silver(I) centres through the pyridinyl N and imine N atoms, with the counter anion out of the coordination sphere. The 4-pyridinyl derivatives conversely gave complexes in which two ligands coordinate to the silver(I) centre through their pyridinyl N atoms only, most likely a linear fashion. The newly synthesized silver(I) complexes and the free ligands were evaluated for their *in vitro* antimicrobial activity against *Escherichia coli*, *Salmonella typhimirium*, *Staphylococcus aureus* and *Candida albicans*. The complexes showed varied growth inhibitory activity against the test organisms.

Keywords: silver(I) complexes, pyridinyl ligands, Schiff base, antimicrobial activity

1.0 Introduction

There is an urgent and sustained pressure on scientists to develop novel and effective antimicrobial agents with minimal cytotoxicity on mammalian cells. This is has been triggered, firstly, by the emergence and rise of multidrug resistant strains of microbes (superbugs) that are progressively becoming less treatable, especially by first choice antibiotics and antiseptics [1, 2]. This has resulted in many clinical antibacterial and antifungal drugs becoming less effective [3] heralding the return of stubborn infections, that are turning fatal.. Moreover, some of the antibacterial and antifungal agents currently in use have undesirable and life threatening side effects thus their usage is deemed counterproductive [4]. The failure and decline of a number of antibiotics available for tackling multidrug resistant strains has occasioned the return to traditional (pre-antibiotic) methods of managing infectious diseases. These include focusing on use of antimicrobial metal based agents, such as silver based products in aiding the fight on infectious diseases [5, 6]. The resurgence on research and application of silver(I) as a premier candidate in fighting infectious diseases is well on course and has been greatly reviewed [6-10]. Pure silver metal is biologically inactive, however in moist conditions, it ionizes readily into silver(I) cations that portray antimicrobial activity. Silver nanoparticles have been hypothesised to show biological activity not only by releasing silver(I) ions, but also by anchoring on and penetrating bacterial cell walls and thus causing structural changes on their cell membranes. This increases permeability into the cell and consequently the cells are destroyed [11]. Moreover, nanosilver particles are also thought to show biological activity by releasing free radicals that in turn induce membrane damage [12]. Silver is well-known medicinal agent owing to its broad spectrum activity at low concentrations against stubborn infectious gram-negative and gram-positive bacteria, fungi and yeast, including antibiotic resistant strains. Additionally, it has been successfully used as a medicinal agent due to its low toxicity and low bio-accumulation in the mammalian body making it a potentially safe internalized therapeutic agent. Silver has been reported to portray multiple modes of action such as; (i) inhibiting activity of some enzymes e.g. those that mediate respiration [13], (ii) binding with DNA cells [13] and (iii) rescinding normal biological activity of bacteria protein by reacting with sensitive thiol groups on the proteins [14]. Specificity on the various modes of action of silver(I) has been explicitly reviewed by S. L. Percivala *et al*., [15].

Traditionally, silver was applied as silver nitrate, however, current research is inclined towards silver based inorganic antimicrobials and silver nanomaterials [16, 17], due to their reduced photosensitivity as well as their potential for controlled release of silver ions. Success of silver based antimicrobials is tied to the ancillary ligands and their ability to stabilize the oxidation state [18]. The ligands also play a key role in modifying the lipophilicity, bioavailability and reactivity of the silver based antimicrobials [19]. The main challenge in designing silver based antimicrobial drugs lies in optimizing slow controlled and sustained release of silver(I) ions over a period of time. Usage of ligands that bond very firmly to the silver(I) centre, could hamper timely release of silver(I) ions. This would essentially result in compromised and reduced antibacterial activity and high risk for silver(I) resistance by the microbes.

Due to the promise of silver in bolstering the fight against infectious diseases, it has been employed in production of various silver coated medical devices [20, 21] and silver-based wound care dressings where elemental silver is incorporated within the dressing rather than being applied as a separate compound or solution [22, 23]. Silver(I) is still being used in modern medicine for the prevention and treatment of bacterial infections associated with second and third degree burns and other open wounds where it is applied as silver sulfadiazine cream [24]. Colloidal silver proteins are being used as mineral supplements though their indiscriminate usage is being discouraged in order to reduce risks leading to agyria [25]. Based on the merits associated with silver(I) and emerging challenges in treatment of diseases, there is a great interest in developing new silver(I) compounds with high pharmacological activity such as antitumor [26-28] and anticancer agents [29, 30], anti-ulcer [31, 32], antibacterial [33, 34], and antifungal [35, 36] properties. This is in the quest to find new drugs to bolster the existing ones and ramp the fight on diseases.

Antibacterial and antifungal studies of silver(I) complexes dominate other biological applications [37]. Silver(I) complexes of N-donor ligands have shown spectacularly a wide spectra antimicrobial activities against bacteria and fungi [38]. For instance, functionalized pyridine derivatives have been used as bactericides [39-41], fungicides [42]. On the other hand, metal free Schiff bases exhibit a broad range of biological activities, including antifungal [43], antibacterial [44, 45], antimalarial [46], anticancer [47, 48], anti-inflammatory [49] and antiviral [50] properties. The imine group is largely credited for the biological activities portrayed by Schiff base compounds [51-53]. With astute design and

synthesis, metal complexes of Schiff base ligands provide good platform of forming new medicinal compounds with good therapeutic activity [52].

In light of aforementioned merits of silver(I), N heterocycles and Schiff base functions, we have designed and synthesised silver(I)-pyridinyl Schiff base complexes for antimicrobial studies. It was hypothesised that these ligands and silver(I) ions would act synergistically and hence show pronounced activity against gram-negative and gram-positive bacteria as well as fungi. The (*E*)-*N*-(pyridinylmethylene)aniline ligands were synthesised *via* mechanochemistry technique under-solvent free conditions. The antimicrobial potency of the new discrete silver(I) complexes with (*E*)-*N*-(pyridinylmethylene)aniline ligands were studied. Also, the influence of subtle changes in the electronic and steric properties of the (*E*)-*N*-(pyridinylmethylene)aniline ligands in biological properties of the silver(I) complexes was investigated. Though silver(I)-pyridinyl Schiff base complexes have been reported before, a huge chunk of these studies focuses on the photoluminescence and structural aspects of silver(I) polymeric or discrete helices obtained by complexing the metal with polydentate pyridinyl Schiff bases [54-62]. Moreover, the pyridinyl Schiff base ligands employed in the reported studies are often synthesised *via* the conventional technique (i.e. reflux method).

2.0 Experimental

2.1 Materials, physical measurements and general procedures

All commercially available chemical reagents and gases were procured from local suppliers and were used without further purification or modification. These were: 2-pyridinecarboxaldehyde 99% (Aldrich, USA), 4-pyridinecarboxaldehyde 97% (Aldrich, USA), 2,2-dimethylaniline 99% (Aldrich), 2,6-diisopropylaniline >92% (Merck, Germany), silver(I) perchlorate 97% (Aldrich USA), silver trifluoromethanesulfonate >99% (Aldrich, USA), dimethyl sulfoxide-d_6 99.8% (Merck, Germany), silver nitrate 99.8% (Aldrich, USA), , argon gas, 5.0 technical grade, (Airflex Industrial Gases, South Africa), nitrogen, 5.0 gas technical grade (Airflex Industrial Gases, South Africa). All solvents employed in the synthesis and work ups i.e. ethanol 99.5% (Associated Chemical Enterprise, South Africa), diethyl ether > 99% (Aldrich), dichloromethane 99% (Aldrich), were dried by standard procedures and distilled under nitrogen prior to use. All manipulations in synthesis of the complexes reported here were performed under an atmosphere of dry argon gas by use of standard Schlenk techniques.

The ^{1}H and ^{13}C NMR spectra were recorded in deuterated DMSO-d_6, on Bruker *AVANCE*^{III} 400 MHz spectrometer. The chemical shifts are reported in ppm relative to the solvent peak shift (2.5 and 39.5 ppm for ^{1}H and ^{13}C NMR respectively). The splitting patterns in ^{1}H NMR spectra are reported as follows: s = singlet, d = doublet, m = multiplet and J values are given in Hertz. FT-IR spectra of the compounds were recorded in the range of 4000 – 400 cm^{-1} regions with a PerkinElmer spectrum 100 FT-IR spectrometer and the data are reported as percentage transmittances at given wavenumbers. High resolution electro-spray ionization (ESI) mass spectrometry spectra were recorded using a Waters Micromass LCT Premier TOF-MS. Only the molecular ions (M^{+}) and the major fragmentation peaks are reported. All melting points were determined using Stuart Scientific melting point apparatus (SMP10). Microanalyses were performed on a Thermoscientific Flash 2000 elemental analyser. Single crystal analysis were done on Bruker Smart APEX2 diffractometer.

2.2 Synthesis of ligands

The ligands (*E*)-*N*-(pyridinylmethylene)aniline numbered **L1** – **L6** (Scheme 1) were synthesised by solvent-less grinding (mechanochemical) of the respective aniline together with appropriate pyridinecarboxaldehyde in a Pyrex tube with a fitted ground joint. Grinding for 2 – 5 min resulted in a paste (**L3**, **L4** and **L6**) or an amber viscous oil (**L1**, **L2** and **L5**). The pastes were left to dry to the desired products in air while the oils were dried under reduced pressure overnight. All the physical and spectral data for the known ligands [63-65] i.e. colour, melting points, IR, ^{1}H and ^{13}C NMR were in line with the ones previously reported (see supporting information) [66, 67].

2.3 Synthesis of complexes

The complexes were prepared by reacting two equivalents of the respective ligands with the appropriate silver(I) salt. Generally, a solution of ligand (either of **L1** – **L6**) in dry ethanol (*ca* 15 mL) was added slowly to a solution of the respective silver salt ($AgClO_4$, AgOTf or $AgNO_3$) in anhydrous ethanol (*ca* 10 ml), while stirring at room temperature. The solution was further stirred for six hours yield to yield precipitates. The obtained solids were then isolated by filtration using Buchner system and recrystallized from dichloromethane/diethyl ether or dichloromethane/hexane. Where precipitates were not obtained, the solvent was removed under reduced pressure and solid obtained recrystallized in dichloromethane/diethyl ether solvent.

2.3.1 $[Ag(L1)_2]ClO_4$, 1

Synthesised by use of (*E*)-*N*-(pyridin-2-ylmethylene)aniline **L1**, (0.3866 2.12 mmol) and silver perchlorate (0.2104 g, 1 mmol). A shiny laser lemon solid obtained (0.5431 g, 95%). Melting point: 149 – 150 °C. ^{1}H NMR (400 MHz, DMSO-d_6, 25℃): δ = 7.34 (d, *J* = 7.2 Hz, 2 H, Hh-C_6H_5), 7.42 (t, *J* = 15.3 Hz, *J* = 7.3 Hz, 4 H, Hg-C_6H_5), 7.48 (d, *J* = 7.9 Hz, 4 H, Hf- C_6H_5), 7.78 (m, 2 H, Hc-C_5H_4N), 8.13 (d, *J* = 7.6 Hz, 2 H, Hd- C_5H_4N), 8.23 (td, *J* = 7.8 Hz, *J* = 1.7 Hz, 2 H, Hc- C_5H_4N), 8.80 (d, *J* = 4.2 Hz, 2 H, Ha- C_5H_4N), 9.09 (s, 2 H, CH=N) ppm. ^{13}C NMR (400 MHz, DMSO-d_6, 25℃): δ = 122.10 (C_6H_5), 128.09 (C_5H_4N), 128.13 (C_6H_5), 128.75 (C_6H_5), 129.46 (C_5H_4N), 139.36 (C_5H_4N), 148.06 (C_5H_4N), 149.77 (C_5H_4N), 151.30 (C_6H_5), 159.91 (CH=N) ppm. FT-IR: 3068, 1590, 1490, 1072, 902 cm^{-1}. MS (ESI-TOF): *m/z* Calcd. for $[Ag(L1)_2]$: 471.0739; found $[M^+]$: 471.0760 (100%), 471.0739 (98%) [AgL1] 289.0114 (28%). Anal. Calcd. (%) for $[Ag(L1)_2]ClO_4$: C, 50.42; H, 3.53; N, 9.80; found (%): C, 50.53; H, 3.29; N, 9.80.

2.3.2 $[Ag(L1)_2]OTf$, 2

Synthesis by use of (*E*)-*N*-(pyridin-2-ylmethylene)aniline **L1**, (0.3866 2.12 mmol) and silver trifluoromethanesulfonate (0.2573 g, 1 mmol) gave a shiny lemon yellow solid obtained, (0.5343 g, 86%). Melting point 136 – 137 °C. ^{1}H NMR (400 MHz, DMSO-d_6, 25℃): δ = 7.34 (t, *J* = 7.1 Hz, 2 H, Hh-C_6H_5), 7.41 - 7.49 (m, 8 H, Hf-, Hg- C_6H_5), 7.76 (td, *J* = 12.3 Hz, *J* = 6.1 Hz, 2 H, Hb-C_5H_4N), 8.13 (d, *J* = 7.6 Hz, 2 H, Hd- C_5H_4N), 8.21 (t, *J* = 15.3 Hz, *J* = 7.6 Hz, 2 H, Hc- C_6H_5), 8.80 (d, *J* = 4.6 Hz, 2 H, Ha- C_5H_4N), 9.03 (s, 2 H, CH=N) ppm. ^{13}C NMR (400 MHz, DMSO-d_6, 25℃): δ = 122.18 (C2- C_6H_5), 128.09 (C4- C_6H_5), 129.58 (C3-C_6H_5), 137.90 (C5- C_5H_4N), 139.36 (C4- C_5H_4N), 151.32 (C1- C_5H_4N, C3- C_5H_4N, C7-C_6H_5), 160.01 (CH=N). FT-IR: 3071, 1589, 1489, 1255, 1151, 1027 cm^{-1}. MS (ESI-TOF): *m/z* Calcd. for $[Ag(L1)_2]$; 471.0739 found: 471.0731 (100%); 470.4012 (10%), 472.0765 (30%), 473.0731 (99%), 474.0764 (30%). Anal. Calcd. (%) for $[Ag(L2)_2]O_3SCF_3$: C, 48.32; H, 3.24; N, 9.02; found (%): C, 48.69; H, 3.24; N, 8.93.

2.3.3 $[Ag(L2)_2]ClO_4$, 3

Synthesised by use of (*E*)-2,6-dimethyl-*N*-(pyridin-2-ylmethylene)aniline (0.4364 g, 2.08 mmol) and silver perchlorate (0.2108 g, 1.02 mmol. A light khaki solid obtained (0. 0.605 g, 94%). Melting point: 202 °C with decomposition. ^{1}H NMR (400 MHz, DMSO-d_6, 25℃): δ

= 2.05 (s, 12 H, Hh-CH_3), 7.05 (t, *J* = 7.4 Hz, 2 H, Hg-C_6H_5), 7.11 (d, *J* = 7.4 Hz, 4 H, Hf-C_6H_5), 7.79 - 7.82 (m, 2 H, Hb-C_5H_4N), 8.05 (d, *J* = 7.6 Hz, 2 H, Hc-C_5H_4N), 8.22 (td, *J* = 7.8 Hz, *J* = 1.7 Hz, 2 H, Hd- C_5H_4N), 8.63 (s, 2 H, He-CH=N), 8.76 (d, *J* = 4.9 Hz, 2 H, Ha-C_5H_4N) ppm. ^{13}C NMR (400 MHz, DMSO-d_6, 25℃): δ = 18.19 (CH_3), 124.93 (C_6H_5), 127.06 (C_5H_4N), 128.09 (C_5H_4N), 128.46 (C_5H_4N), 139.45 (C5- C_5H_4N), 148.80 (C_5H_4N, C_6H_5), 151.11 (C_5H_4N), 163.94 (CH=N). FT-IR: 3068, 2913, 1639, 1591, 1468, 1442, 1265, 1301, 1061, 900 cm^{-1}. MS (ESI-TOF): *m/z* Calcd. for [Ag(L2)$_2$]: 527.1365; found: 527.1376 (100%), 528.1409(30%). 529.1375(100%), 530.1525(30%), [AgL2], 317.0292(85%), 319.0288(80%). Anal. Calcd. (%) for [Ag(L2)$_2$]ClO_4: C, 53.56; H, 4.49; N, 8.92; found (%): C, 53.46; H, 4.10; N, 8.92.

2.3.4 [Ag(L2)$_2$]OTf, 4

Synthesised by use of (*E*)-2,6-dimethyl-*N*-(pyridin-2-ylmethylene)aniline (0.4224 g, 2.00 mmol) and silver trifluoromethanesulfonate (0.2352 g, 0.91 mmol). Banana yellow solid (0.5691 g, 92%). Crystals for single crystal X ray diffraction analysis were obtained by layering diethyl ether onto dichloromethane solution of product. Melting point 183 - 184 °C. ^{1}H NMR (400 MHz, DMSO-d_6, 25℃): δ = 2.00 (s, 12 H, Hh-CH_3), 7.00 (t, *J* = 6.3 Hz, 2 H, Hg- C_6H_5), 7.07 (d, *J* = 7.3 Hz, 4 H, H-C_6H_3), 7.75 (t, *J* = 6.0 Hz, 2 H, Hb-C_5H_4N), 8.08 (d, *J* = 7.7 Hz, 2 H, Hd-C_5H_4N), 8.16 (td, *J* = 7.6 Hz, *J* = 1.6 Hz, 2 H, Hc-C_5H_4N), 8.57 (s, 2 H, He-CH=N), 8.71 (d, *J* = 4.5 Hz, 2 H, Ha-C_5H_4N) ppm. ^{13}C NMR (400 MHz, DMSO-d_6, 25℃): δ = 17.79 (CH_3), 124.73 (C_5H_4N), 126.85 (C_5H_4N), 127.14 (C10- C_6H_5), 127.98 (C8-, C12- C_6H_5), 128.07 (C_6H_5), 139.03 (C_5H_4N), 148.98 (C_5H_4N), 149.76 (C_6H_5), 150.82 (C_5H_4N), 163.94 (CH=N) ppm. FT-IR: 2942, 1639, 1591, 1474, 1442, 1258, 1149, 1090, 1030 cm^{-1}. MS (ESI-TOF) *m/z*: Calcd. for [Ag(L2)$_2$]: 527.1365 Found [M$^+$]: 527.1360(100%) 527.1091(98%) 530.1127(30%). Anal. Calcd. (%) for [Ag(L2)$_2$]O_3SCF_3: C, 51.41; H, 4.17; N, 8.27; found (%): C, 51.67; H, 3.85; N, 8.17.

2.3.5 [Ag(L2)$_2$]NO_3, 5

Synthesised by use of silver nitrate (0.1700 g, 1.0 mmol) and (*E*)-2,6-dimethyl-*N*-(pyridin-2-ylmethylene)aniline **L2**, (0.4204 g, 2.00 mmol). A golden yellow solid (0.5488 g, 93%). Melting point 190 – 191 °C. ^{1}H NMR (400 MHz, DMSO-d_6, 25℃): δ = 1.97 (s, 12 H, Hh-CH_3), 7.01 (t, *J* = 8.8 Hz, *J* = 5.9 Hz, 2 H, Hg-C_6H_3), 7.06 (d, *J* = 6.4 Hz, 4 H, Hf-C_6H_3), 7.77 (t, *J* = 12.5 Hz, J = 6.0 Hz, 2 H, Hb-C_5H_4N), 8.06 (d, *J* = 7.7 Hz, 2 H, Hd-C_5H_4N), 8.20 (td, *J*

= 7.6 Hz, *J* = 1.6, 2 H, Hc-C_5H_4N), 8.61 (s, 2 H, He-CH=N), 8.69 (d, *J* = 4.2 Hz, 2 H, Ha-C_5H_4N) ppm. ^{13}C NMR (400 MHz, DMSO-d_6, 25℃): δ = 17.75 (CH_3), 124.87, (C_5H_4N), 126.94 (C_5H_4N), 128.08 (C_6H_3), 128.30 (C_6H_3), 139.31 (C_5H_4N), 148.80 (C_5H_4N), 149.17 (C_5H_4N), 150.99 (C_5H_4N), 163.99 (CH=N) ppm. FT-IR: 3061, 2958, 2909, 1646, 1592, 1337, 1187, 772 cm^{-1}. MS (ESI-TOF): *m/z* Calcd. for [Ag(L2)$_2$]: 527.1365; found 527.1375(10%), 528.1411(30%), 529.1375 (100%), 530.1407(30%), [AgL2] 317.0423 (70%). Anal. Calcd. (%) for [Ag(L2)$_2$]NO_3: C, 56.96; H, 4.78; N, 11.86; found (%): C, 56.96; H, 4.50; N, 11.81.

2.3.6 [Ag(L3)$_2$]ClO_4, 6

Synthesised by use of (*E*)-2,6-diisopropyl-N-(pyridin-2-ylmethylene)aniline **L3**, (0.5321 g, 2.00 mmol) and silver perchlorate (0.2028 g, 0.98 mmol). A laser lemon solid obtained, (0.690 g, 95%). Melting point 250 – 251 °C. ^{1}H NMR (400 MHz, DMSO, d_6, 25℃): δ = 0.99 (d, *J* = 6.8 Hz, 24 H, Hi-CH_3), 2.91 (t, *J* = 6.8 Hz, 4 H, Hh-$CH(CH_3)_2$), 7.17 (s, 6 H, He,Hf-C_6H_5), 7.64 - 7.68 (m, 2 H, Hc-C_5H_4N), 8.11 (d, *J* = 7.12 Hz, 2 H, Hd-C_5H_4N), 8.15 (td, *J* = 7.7 Hz, *J* = 1.6 Hz, 2 H, Hb-C_5H_4N), 8.40 (d, *J* = 4.6 Hz, 2 H, Ha-C_5H_4N), 8.59 (s, 2 H, CH=N) ppm. ^{13}C NMR: (400 MHz, DMSO-d_6, 25℃) δ = 23.10 (CH_3), 27.45 ($CH(CH_3)_2$), 123.04 (C_6H_5), 125.25 (C_6H_5), 127.00 (C_5H_4N), 127.85 (C_5H_4N), 137.08 (C_5H_4N), 139.02 (C_6H_5), 147.04 (C_6H_5), 149.60 (C_5H_4N), 150.50 (C_5H_4N), 163.36 (CH=N). FT-IR: 3067, 3026, 2960, 2879, 1636, 1592, 1444, 1061, 900 cm^{-1}. MS (ESI-TOF) *m/z*: Calcd. for [Ag(L3)$_2$] 639.2617 found 639.2643(100%), 641.2651(40%), 640.2686(100%) [AgL3] 373.0828(25%). Anal. Calcd. (%) for [Ag(L3)$_2$]ClO_4: C, 58.42; H, 5.99; N, 7.57; found (%): C, 58.33; H, 5.71; N, 7.78.

2.3.7 [Ag(L3)$_2$]OTf, 7

Synthesised by use of (*E*)-2,6-diisopropyl-*N*-(pyridin-2-ylmethylene)aniline **L3** (0.474 g, 1.77 mmol) and silver trifluoromethanesulfonate (0.2160 g, 0.84 mmol). An aureolin solid obtained (0.6244 g, 94%). Crystals for single crystal X-ray diffraction were obtained by slow evaporation of the ethanol solution of the solid. Melting point 240 – 241 °C. ^{1}H NMR (400 MHz, DMSO-d_6, 25℃): δ = 0.99 (d, *J* = 6.8 Hz, 24 H, Hi-CH_3), 2.85 (t, *J* = 6.8 Hz, 4 H, Hh-$CH(CH_3)_2$), 7.17 (s, 6 H, Hf-, Hg-C_6H_3), 7.66 (t, *J* = 6.6 Hz, 2 H, Hb-C_5H_4N), 8.11 (d, *J* = 7.2 Hz, 2 H, Hd-C_5H_4N), 8.15 (t, *J* = 15 Hz, J = 7.2 Hz, 2 H, Hc- C_5H_4N), 8.38 (d, *J* = 4.5 Hz, 2 H, Ha-C_5H_4N). 8.6 (s, 2 H, He-CH=N) ppm. ^{13}C NMR (400 MHz, DMSO-d_6, 25℃): δ =

23.09 (CH_3), 27.45 ($CH(CH3)_2$), 123.05 (C_6H_3), 125.29 (C_5H_4N), 127.17 (C_5H_4N), 127.90 (C_6H_3), 137.07 (C_5H_4N), 147.00 (C_6H_3), 149.52 (C_5H_4N), 150.52 (C_5H_4N), 163.35 (CH=N) ppm. FT-IR: 3067, 3028, 2960, 2868, 1638, 1593, 1461, 1446, 1365, 1273, 1254, 1156, 1145, 1028 cm^{-1}. ESI-TOF *m/z*: Calcd. for $[Ag(L2)_2]$: 639.2617 Found: 639.3106 (100 %), 642.3143. Anal. Calcd. (%): C, 56.27; H, 5.62; N, 7.09; found: C, 56.71; H, 6.03; N, 7.51.

2.3.8 $[Ag(L3)_2]NO_3$, 8

Synthesised by use of silver nitrate (0.1712 g 1 mmol) and (*E*)-2,6-diisopropyl-*N*-(pyridin-2-ylmethylene)aniline **L3**, (0.2723 g, 1.03 mmol). Golden yellow solid obtained, (0.400 g, 92%). Melting point: 156 °C with decomposition. ^{1}H NMR (400 MHz, DMSO-d_6, 25℃): δ = 1.03 (d, *J* = 6.9 Hz, 12 H, Hi-CH_3), 2.87 (t, *J* = 13.7 Hz, *J* = 6.8 Hz, 2 H, Hh-$CH(CH_3)_2$), 7.18 (s, 3 H, Hf-, Hg-C_6H_3), 7.71 (t, *J* = 12.2 Hz, *J* = 6.1 Hz, 1 H, Hb-C_5H_4N), 8.12 (d, *J* = 7.5 Hz, 1 H, Hd-C_5H_4N), 8.17 (t, *J* = 15.1 Hz, J = 7.6 Hz, Hc- C_5H_4N), 8.52 (d, *J* = 4.4 Hz, 1 H, Ha-C_5H_4N), 8.61 (s, 1 H, He-CH=N) ppm. ^{13}C NMR (400 MHz, DMSO-d_6, 25℃): δ = 23.18 (CH_3), 27.44 ($CH(CH_3)_2$), 123.05, (C_6H_3), 125.26 (C_6H_3), 127.95 (C_5H_4N), 137.15 (C_6H_3), 139.11 (C_5H_4N), 147.06 (C_6H_3), 150.68 (C_5H_4N), 163.36 (CH=N) ppm. FT-IR: 3025, 2964, 1637, 1591, 1407, 1363, 1290, 1176, 781 cm^{-1}. MS (ESI-TOF) *m/z*: Calcd. for $[Ag(L3)_2]$: 639.2617 found $[M^+]$ 639.2624 (100%), 641.2627; [AgL3] 373.0078(25%). Anal. Calcd. (%) for $[AgL3]NO_3$: C, 49.56; H, 5.08; N, 9.63; found (%): C, 49.26; H, 4.57; N, 9.53.

2.3.9 $[Ag(L4)_2]ClO_4$, 9

Synthesised by use of (*E*)-*N*-(pyridin-4-ylmethylene)aniline **L4**, (0.3585 g, 1.97 mmol) and silver perchlorate (0.1930 g, 0.93 mmol). An off white solid obtained (0.4820 g 91%). Melting point 190 - 191 °C. ^{1}H-NMR (400 MHz, DMSO-d_6, 25℃): δ = 7.30 (d, 2 H, *J* = 7.2 Hz, Hf-C_6H_5), 7.34 (d, 4 H, *J* = 7.3 Hz, He-C_6H_5), 7.45 (d, 4 H, *J* = 7.5 Hz, Hd-$_6H_5$), 7.93 (d, 4 H, *J* = 6 Hz, Hb-C_5H_4N), 8.71 (s, 2 H, Hc-CH=N), 8.77 (d, 4 H, *J* = 6.0 Hz, Ha-C_5H_4N) ppm. ^{13}C-NMR (400 MHz, DMSO-d_6, 25℃): δ = 121.66 (C_5H_4N), 122.75 (C_6H_5) 127.94 (C_6H_5), 129.76 (C_6H_5), 143.46 (C_5H_4N), 151.25 (C_5H_4N), 151.74 (C_5H_4N), 159.46 (CH=N) ppm. FT-IR: 3052, 1612, 1424, 1067, 926 cm^{-1}. MS (ESI-TOF) *m/z*: $[Ag(L4)_2]$: 471.0739 found $[M^+]$: 471.0760 [AgL4] 289.0114(28%). Anal. Calcd. (%) for $[AgL_2]ClO_4$. C, 50.42; H, 3.53; N, 9.80; found (%): C, 50.73; H, 3.36; N, 9.69.

2.3.10 $[Ag(L5)_2]ClO_4$, 10

Synthesised by use of (*E*)-2,6-dimethyl-*N*-(pyridin-4-ylmethylene)aniline **L5**, (0.4410 g, 2.10 mmol) and $AgCLO_4$ (0.2131 g, 1.03 mmol). An electric yellow solid (0.530 g, 82%). Melting point 210 °C. ^{1}H NMR (400 MHz, DMSO-d_6, 25℃): δ = 2.07 (s, 12 H, Hf-CH_3), 6.97 (t, *J* = 15 Hz, *J* = 7.3 Hz, 2 H, He-C_6H_5), 7.08 (d, *J* = 7.6 Hz, 4 H, Hd-C_6H_5), 7.92 (d, *J* = 5.7 Hz, 4 H, Hb-C_6H_5), 8.43 (s, 2 H, Hc-CH=N), 8.78 (d, *J* = 5.6 Hz, 4 H, Ha-C_5H_4N). ^{13}C NMR (400 MHz, DMSO-d_6, 25℃): δ = 17.82 (CH_3), 124.03 (C_6H_5), 126.18 (C_6H_5), 127.97 (C_6H_5), 142.57 (C_5H_4N), 150.10 (C_6H_5), 150.83 (C_5H_4N), 162.08 (CH=N). FT-IR: 2920, 1613, 1469, 1426, 1076, 924 cm^{-1}. MS (ESI-TOF): *m/z*, Calcd. for $[Ag(L5)_2]$: 527.1365 found: 527.1680(100%), 527.1516(40%), [AgL5] 317.0304(100%), 319.0305(95%). Anal. Calcd. (%) for $[Ag(L5)_2]ClO_4$: C, 53.56; H, 4.49; N, 8.92; found (%): C, 53.63; H, 4.10; N, 8.86.

2.3.11 $[Ag(L5)_2]OTf$, 11

Synthesised by use of (*E*)-2,6-dimethyl-*N*-(pyridin-4-ylmethylene)aniline **L5**, (0.4180 g, 2.00 mmol) and silver trifluoromethanesulfonate (0.2502 g, 0.97 mmol). A lemon precipitate (0.5641 g, 86%). Melting point: 140 -142 °C. ^{1}H NMR (400 MHz, DMSO-d_6, 25℃): δ = 2.06 (s, 12 H, Hf-CH_3), 6.96 (t, *J* = 7.5 Hz, 2 H, H_e-C_6H_5), 7.08 (d, *J* = 7.5 Hz, 4 H, H_d-C_6H_5), 7.89 (d, *J* = 5.8 Hz, 4 H, H_b-C_5H_4N), 8.42 (s, 2 H, CH=N), 8.78 (d, *J* = 5.8 Hz, 4 H, H_a-C_5H_4N) ppm. ^{13}C NMR (400 MHz, DMSO-d_6, 25℃): δ = 17.82 (CH_3), 122.05 (C_5H_4N), 123.99 (C_6H_3), 126.17 (C_6H_3), 127.96 (C_6H_3), 142.38 (C_5H_4N), 150.14 (C_6H_3), 150.65 (C_5H_4N), 162.13 (CH=N). FT-IR: 3061, 2960, 1615, 1284, 1232, 1158, 1026, 825, 630 cm^{-1}. (MS) ESI-TOF *m/z* Calcd. for $[Ag(L5)_2]$: 527.1365; found: 527.1385(100%), [AgL5] 317.0272(12%). Anal. Calcd. for $[Ag(L5)_2]O_3SCF_3$: C, 51.41; H, 4.17; N, 8.27; found: C, 51.67; H, 3.76; N, 7.88.

2.3.12 $[Ag(L5)_2]NO_3$, 12

Synthesised by use of silver nitrate (0.16960, 1.0 mmol) and (*E*)-2,6-dimethyl-*N*-(pyridin-4-ylmethylene)aniline **L5** (0.4300 g, 2.04 mmol). Bumblebee yellow solid, (0.500 g, 85%). Melting point 157 °C with decomposition. ^{1}H NMR (400 MHz, DMSO-d_6, 25℃): δ = 2.07 (s, 12 H, Hf-CH_3), 6.97 (t, *J* = 15 Hz, *J* = 7.5 Hz, 2 H, He-C_6H_3), 7.09 (d, *J* = 7.5 Hz, 4 H, hd-C_6H_3), 7.91 (d, *J* = 6.0 Hz, 4 H, Hb-C_5H_4N), 8.43 (s, 2 H, Hc-CH=N), 8.78 (d, *J* 6.0 Hz, Ha-

C_5H_4N) ppm. ^{13}C NMR (400 MHz, DMSO-d_6, 25℃): δ = 17.82 (CH_3), 122.11 (C_6H_3) 124.00 (C_5H_4N), 126.18 (C_6H_3), 127.96 (C_6H_3), 142.48 (C_5H_4N), 150.13 (C_6H_3), 150.74 (C_5H_4N), 162.11 (CH=N) ppm. FT-IR: 3064, 2960, 1612, 1328, 1175, 764 cm^{-1}. MS (ESI-TOF): *m/z* calcd. for $[Ag(L5)_2]$: 527.1365; found: 527.1365 (100%), 529.1370(100%), 530.1405(30%) Anal. Calcd. (%) for $[Ag(L5)_2]NO_3$: C, 56.96; H, 4.78; N, 11.86; found (%): C, 56.82; H, 4.60; N, 11.77.

2.3.13 $[Ag(L6)_2]ClO_4$ 13

Synthesised by use of (*E*)-2,6-diisopropyl-*N*-(pyridin-4-ylmethylene)aniline **L6** (0.5390 g, 2.02 mmol) and silver perchlorate (0.2100 g, 1.01 mmol). A cream solid obtained, (0.7116 g, 95%). Melting point: 241 °C with decomposition. ^1H NMR (400 MHz, DMSO-d_6, 25℃): δ = 1.11 (d, *J* = 6.9 Hz, 24 H, Hg-CH_3), 2.81 (t, *J* = 13.7 Hz, *J* = 6.9 Hz, 4 H, Hf-$CH(CH_3)_2$), 7.11 (t, *J* = 8.8, *J* = 6.2 Hz, 2 H, Hd -C_6H_3), 7.16 (d, *J* = 6.6 Hz, 4 H, Hc-C_6H_3), 7.89 (d, *J* = 5.9 Hz, 4 H, Hb-C_6H_3N), 8.40 (s, 2 H, CH=N), 8.78 (d, *J* = 5.8 Hz 4 H, Ha-C_6H_3N). ^{13}C NMR (400 MHz, DMSO-d_6, 25℃): δ = 23.15 (CH_3), 27.48 ($CH(CH_3)_3$), 122.27 (C_5H_4N), 122.92 (C_6H_3), 124.50 (C_6H_3), 136.49 (C_6H_3), 142.37 (C_6H_3), 148.28 (C_5H_4N), 151.00 (C_5H_4N), 161.73(CH=N). FT-IR: 2962, 1639, 1614, 1526, 1462, 1427, 1320, 1061, 934 cm^{-1}. MS (ESI-TOF) *m/z*: calcd. for $[Ag(L6)_2]$: 639.2617; found: 639.2623 (98%), 640.2673(30%), 641.2650(100%), 642.2075(30%). Anal. Calcd. (%) for $[Ag(L6)_2]ClO_4$: C, 58.42; H, 5.99; N, 7.57; found (%): C, 58.32; H, 5.77; N, 7.12.

2.3.14 $[Ag(L6)_2]OTf$, 14

Synthesised by use of silver trifluoromethanesulfonate (0.2300 g, 0.90 mmol) and (*E*)-2,6-diisopropyl-*N*-(pyridin-4-ylmethylene)aniline **L6** (0.5040 g, 1.89. A lemon yellow solid, (0.6511 g, 92%). Melting point 238 °C with decomposition. ^1H NMR (400 MHz, DMSO-d_6, 25℃): δ = 1.12 (d, *J* = 6.8 Hz, 24 H, Hg-CH_3), 2.82 (t, *J* = 13.7 Hz, *J* = 6.9 Hz, 4 H, Hf-$CH(CH_3)_2$), 7.11 (t, *J* = 8.8 Hz, Hz, 6.2 Hz, 2 H, He-C_6H_3), 7.17 (t, *J* = 8.8 Hz, *J* = 2 Hz, 4 H, Hd-C_6H_3), 7.91 (d, *J* = 5.9 Hz, 4 H, Hb-C_5H_4N), 8.41 (s, 2 H, Hc-CH=N), 8.78 (d, *J* = 5.9 Hz, 4 H, Ha-C_5H_4N) ppm. ^{13}C NMR (400 MHz, DMSO-d_6, 25℃): δ = 22.58 (CH_3), 27.45 ($CH(CH_3)_2$), 122.88 (C_6H_3), 124.46 (C_5H_4N), 136.47 (C_6H_3), 142.23 (C_6H_3), 148.26 (C_6H_3), 150.76 (C_5H_4N), 151.18 (C_5H_4N), 161.72 (CH=N) ppm. FT-IR: 3062, 2963, 2863, 1638, 1610, 1441, 1422, 1287, 1237, 1159, 1026 cm^{-1}. Anal. Calcd. (%) for $[Ag(L6)_2]O_3SCF_3$: C,

56.27; H, 5.62; N, 7.09; found (%): C, 56.70; H, 5.80; N, 7.27. MS (ESI-TOF): *m/z* calcd. for $[Ag(L6)_2]$: 639.2617; found: 639.2640 (98%), 641.2637 (100%), 642.2671(40%).

2.3.15 $[Ag(L6)_2]NO_3$, 15

Synthesised by use of (*E*)-2,6-diisopropyl-*N*-(pyridin-4-ylmethylene)aniline **L6**, (0.2712 g, 1.02 mmol), and silver nitrate (0.0852 g, 0.5 mmol). Banana yellow solid, (0.31 g, 88%). Melting point: 231 °C with decomposition. ^{1}H NMR (400 MHz, DMSO-d_6, 25℃): δ = 1.10 (d, *J* = 6.8 Hz, 24 H, Hg-CH_3), 2.81 (t, *J* = 13.7 Hz, *J* = 6.8 Hz, 4 H, Hf-$CH(CH_3)_2$), 7.11 (t, *J* = 8.8 Hz, *J* = 6.2 Hz, 2 H, He-C_6H_3), 7.16 (d, *J* = 6.6 Hz, 4 H, Hd-C_6H_3), 7.93 (d, *J* = 6.0 Hz, 4 H, Hb-C_5H_4N), 8.42 (s, 2 H, Hc-CH=N), 8.78 (d, *J* = 6.0 Hz, Ha-C_5H_4N) ppm. ^{13}C NMR (400 MHz, DMSO-d_6, 25℃): 23.15 (CH_3), 27.48 ($CH(CH_3)_2$), 122.26 (C_6H_3), 122.92 (C_6H_3), 124.50 (C_5H_4N), 136.49 (C_6H_3), 142.37 (C_6H_3), 148.28 (C_5H_4N), 151.0 (C_5H_4N), 161.73 (CH=N) ppm. FT-IR: 3050, 2958, 1609, 1305, 817, 765 cm^{-1}. MS (ESI-TOF): *m/z* calcd. for $[Ag(L6)_2]$: 639.2617; found: 639.2624(98%), 641.2627(100%), 642.2661(40%), [AgL6] 373.0078. Anal. Calcd. (%) for $[Ag(L6)_2]NO_3$: C, 61.54; H, 6.31; N, 9.97; found (%): C, 61.92; H, 6.30; N, 9.95.

2.4 Crystal structure determination and refinement

Single crystals suitable for analysis by X-ray diffraction were selected and glued onto the tips of glass fibre mounted on brass holders. Crystal evaluation and data collection were done on a Bruker Smart APEX2 diffractometer with graphite monochromated Mo Kα radiation (λ = 0.71073 Å) equipped with an Oxford Cryostream low temperature apparatus operating at 100 K. The initial cell matrix was determined from three series of scans containing twelve frames collected at intervals of 0.5° in a 6° range with the exposure time of ten seconds per frame and the reflections indexed using the *APEX2* program suite [68]. Data collection involved the use of □ scans of 0.5° width with 20 seconds exposure time per frame. The total number of images was based on results from the program *COSMO*, whereby the expected redundancy was to be 4.0 and completeness of 100% out to 0.75 Å. Cell parameters were retrieved using *APEX2* and refined using *SAINT* on all observed reflections. Data reduction was performed using the *SAINT* [68] software and the scaling and absorption corrections were applied using *SADABS* [69] multi-scan technique. The structure were solved by the direct method using the *SHELXS* program and refined [69]. The visual crystal structure analysis was performed using *ORTEP*-3 system software [70]. Non-hydrogen atoms were first refined isotropically and

then by anisotropic refinement with full-matrix least squares method based on F^2 using *SHELXL* [69]. All hydrogen atoms were positioned geometrically, allowed to ride on their parent atoms and refined isotropically. All the data was subjected to the online checkCIF evaluation criteria. The crystal data and structural refinement information are summarized in Table 1.

Table 1. Crystal data and structure refinement for complexes **4** and **7**

	[Ag(L2)$_2$]OTf, 4	**[Ag(L3)$_2$]OTf, 7**
Empirical formula	C_{18} H_{22} Ag F_3 N_2 O_3 S	C_{37} H_{44} Ag F_3 N_4 O_3 S
Formula weight	511.30	789.69
Temperature	173(2) K	173(2) K
Wavelength	0.71073 Å	0.71073 Å
Crystal system	Monoclinic	Triclinic
Space group	P 21/c	P -1
Unit cell dimensions	a = 16.7539(7) Å	a = 9.041(5) Å
	b = 15.6733(7) Å	b = 11.109(5) Å
	c = 22.8836(10) Å	c = 19.039(5) Å
Volume	5994.1(5) Å^3	1870.5(14) Å^3
Z	8	2
Density (calculated)	1.700 Mg/m^3	1.402 Mg/m^3
Absorption coefficient	1.162 mm^{-1}	0.650 mm^{-1}
F(000)	3096	816
Crystal size (mm^3)	0.430 x 0.280 x 0.260	0.380 x 0.332 x 0.305
Theta range for data collection	1.576 to 27.355°	1.083 to 28.538°
Index ranges	-21 ≤ h≤21,	-11 ≤h ≤ 12,
	-20 ≤k ≤ 20,	-14 ≤ k ≤ 14,
	-29 ≤ l ≤ 29	-25 ≤ l ≤ 25
Reflections collected	100039	40390
Independent reflections	13184 [R(int) = 0.0252]	9333 [R(int) = 0.0256]
Completeness to theta = 25.242°	98.3 %	100.0 %
Refinement method	Full-matrix least-squares on F^2	Full-matrix least-squares on F^2
Data / restraints / parameters	13184 / 0 / 747	9333 / 0 / 442
Goodness-of-fit on F^2	1.153	1.127
Final R indices [I > 2 sigma (I)]	R1 = 0.0294, wR2 = 0.0695	R1 = 0.0233, wR2 = 0.0649
R indices (all data)	R1 = 0.0360, wR2 =	R1 = 0.0258, wR2 =

	0.0754	0.0718
Extinction coefficient	n/a	n/a
Largest diff. peak and hole (Å^{-3})	0.869 and -0.614	0.496 and -0.520

2.5 Biological studies

2.5.1 Inoculation procedure

Inoculation of the microorganism used was done in nutrient broth after sterilization. Nutrient broth (1.3 g) was dissolved in distilled water (100 mL). The nutrient broth, *ca* 10 mL, was poured into test tubes. The test tubes were plugged with cotton wool and then wrapped with aluminium foil. The broth in test tubes was sterilized by autoclaving at 121 °C for 15 min and then allowed to cool to 37 ℃. Thereafter the microorganisms were inoculated using sterilized cotton swabs. The inoculums were incubated at 37 ℃ for 24 hr.

2.5.2 Preparation of Müeller-Hinton agar test plates

Müeller-Hinton agar (38 g) was dissolved in distilled water (1 L) and the resulting agar medium was sterilized by autoclaving at 121 °C for 15 min. The medium was allowed to cool in a water bath set at 45 °C. Approximately 25 mL of the cool agar medium were poured into sterile flat-bottomed glass petri dishes to give a uniform depth of approximately 4 mm. The agar medium was allowed to cool to room temperature (*ca*. 25 °C) and set. The test organisms were then struck on the surface of the agar medium using sterile wire loops. The paper discs containing the 20 μg of compound under investigation were then loaded onto the already-inoculated agar plates using sterilized forceps and then incubated at 37 ℃ for 24 hr. The diameters of the inhibition zones around the disc were measured. Each compound was screened in triplicate and three independent experiments were performed. The minimum inhibitory concentrations were determined through the agar dilution method.

A representative sample of each batch of plates without any microorganism was also incubated at the same temperature for 24 hr to examine for sterility. Viability of the organisms was tested by incubating test plates without the compounds being investigated. Chloramphenicol was used as the standard antibacterial agent whereas fluconazole was used in the technique as the standard antifungal agent.

3.0 RESULTS AND DISCUSSION

3.1 Synthesis and characterisation of ligands

A series of pyridinyl derived Schiff bases (**L1 – L6**) were synthesised by an equimolar condensation reaction between substituted aromatic anilines and pyridinealdehydes *via* mechanochemical approach (Scheme 1) where, the appropriate reactants were ground together neat for approximately 2 – 5 min then products dried under reduced pressure or in air to remove the water produced in the reaction. The ligands were obtained as amber oils or light yellow solids. The ligands were characterised by melting point (where applicable), IR, ^{1}H NMR, ^{13}C NMR, and mass spectrometry. The absence of the aldehydic carbonyl stretching bands (1720 – 1740 cm^{-1}) and primary amine N-H stretching bands (3400 – 3500 cm^{-1}), and a corresponding appearance of the characteristic azomethine VC=N sharp bands ranging from to 1630 to 1640 cm^{-1}, confirmed the formation of the Schiff bases. This conforms well to reported data of the relevant compounds [67]. The relatively weak absorption bands ranging from 3020 - 3070 cm^{-1} in the ligands are due to the C–H modes involving the aromatic ring hydrogen atoms. The C–H modes involving the aliphatic hydrogen atoms in **L2**, **L3**, **L5** and **L6** appear at 2915, 2959, 2917 and 2960 cm^{-1}, respectively. The absorption bands with variable intensity in the frequency range 1410–1590 cm^{-1} correspond to ring vibrations of the pyridinyl rings of the ligands. Other bands with various intensity below 1400 cm^{-1} are due to the C–C vibrations, C–H bending and C–N stretching.

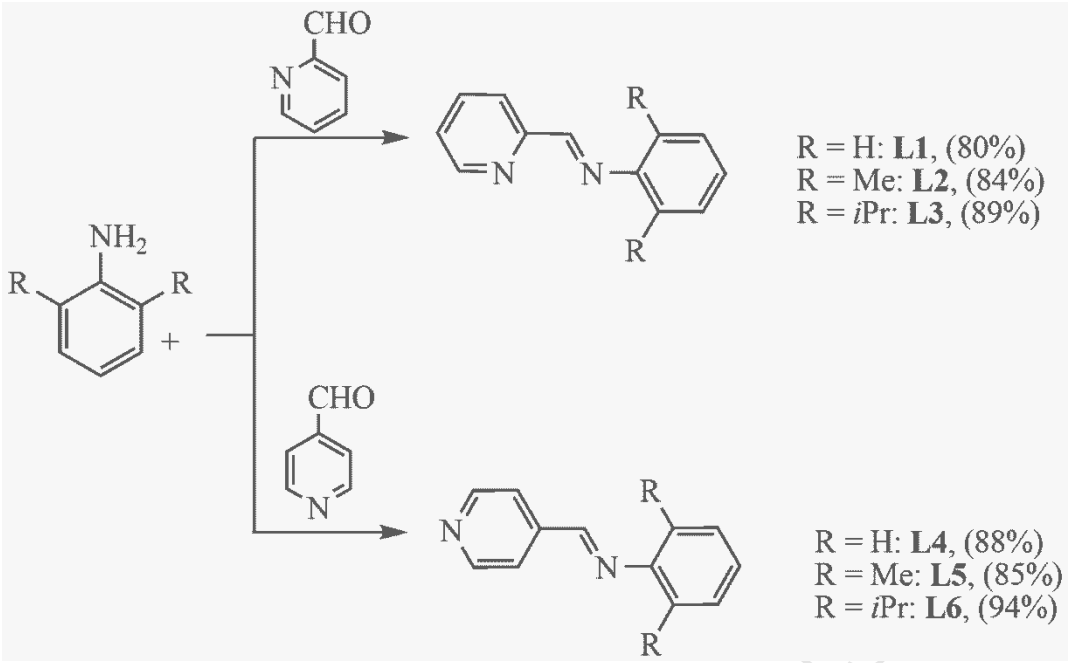

Scheme 1: Solvent-free synthesis of the ligands in air at room temperature *via* mechanochemistry technique. Yields are provided in parentheses.

The ^{1}H NMR spectra of each ligand **L1** – **L6**, in deuterated DMSO-d_6 exhibited a singlet at 8.59, 8.29, 8.26, 8.67, 8.40 and 8.40 ppm respectively. These peaks are assigned to the resonance of the azomethine (CH=N) proton. In general, the aromatic proton signals appear at *ca* 7.00 – 8.78 ppm in the ^{1}H NMR spectra of these ligands. A singlet at 2.06 ppm indicates the presence of methyl groups in **L2** and **L5**; a doublet at *ca* 1.10 ppm and a triplet at *ca* 2.86 (**L3**) and 2.82 (**L6**) indicates presence of the isopropyl groups in **L3** and **L6**. The protons on alpha carbons with respect to N atoms are summarized in Table 2.

Table 2: ^{1}H NMR chemical shifts of some protons in the **L1** – **L6** in DMSO-d_6

Compound	**CH=N**	**Ha-C_5H_4N**	**Hb-C_5H_4N**
L1	8.59	8.71	7.50
L2	8.29	8.71	753
L3	8.26	8.72	7.56
L4	8.67	8.75	7.85
L5	8.40	8.77	7.87
L6	8.40	8.77	7.88

3.2 Synthesis and characterisation of the of complexes

Coordination of the silver(I) by the ligands was achieved by stirring one equivalent of a silver(I) salt with 2 equivalents of a ligand in anhydrous ethanol at room temperature under dry argon for 6 to 12hr. All complexes from silver perchlorate formed precipitates within 10 min of the reaction. The FT-IR spectrum of the complexes show some fundamental differences when compared with those of the free ligands. The stretching frequency bands at 1590, 1589, 1591, 1591, 1592, 1592, 1593, 1591 in the FTIR spectra of complexes **1** – **8**, respectively, corresponds $_{V}$C=N imine bond stretching. These bands in the complexes are red shifted to lower wavenumbers relative to comparable bands in free ligands. This is a strong indicator that the N_{im} donor participates in coordination of the silver(I) atoms. The red shift upon coordination is in conformity to what has been observed elsewhere for silver(I)-N_{im} coordination [55, 71]. The FTIR spectral data results provide strong evidences for the complexation of the pyridinyl Schiff bases **L1** – **L3** coordinate *via* both pyridinyl and imine N atoms and also suggests that the complexes exist as discrete cationic complexes in the solid state [72]. The stretching peaks for $_{V}$C=N imine bond in complexes **9** – **15** appear at the same position like in the corresponding free ligands (either **L4** – **L6**). The fact that these bands do no shift indicates that the imine N atoms in complexes **9** – **15** are not involved in the coordination of silver(I) ions. The peaks at 1072, 1061, 1083, 1067, 1076 and 1061 cm^{-1} in complexes **1**, **3**, **6**, **9**, **10** and **13** correspond to the v_3 asymmetric stretch of free perchlorate anions whereas respective peaks at 902, 900, 932, 926, 924 and 934 cm^{-1} correspond to the V_1 asymmetric stretching in the free perchlorate anions [73]. The peaks at 1271, 1258, 1254 and 1237 cm^{-1} in the spectra of complexes **2**, **4**, **7** and **11**, respectively, are for the degenerate antisymmetric stretch of the SO_3 moiety in free trifluoromethanesulfonate anions. The peaks at 1027, 1030, 1028 and 1026 cm^{-1} are assigned the symmetric stretching in SO_3 moiety in the triflate anion accompanying the respective complexes. Also, the degenerate antisymmetric stretch of the CF_3 moiety are observed at 1151, 1149, 1156 and 1159 cm^{-1}, respectively [74]. The sharp strong peaks at 1290 – 1337 cm^{-1} in the IR spectra of complexes **5**, **8**, **12** and **15** are assigned to the nitrate anion vibration modes which agrees well with related compounds [56, 75-77]. The absorption bands with variable intensity in the frequency range 1422 – 1490 cm^{-1} correspond to the pyridinyl ring vibrations [57].

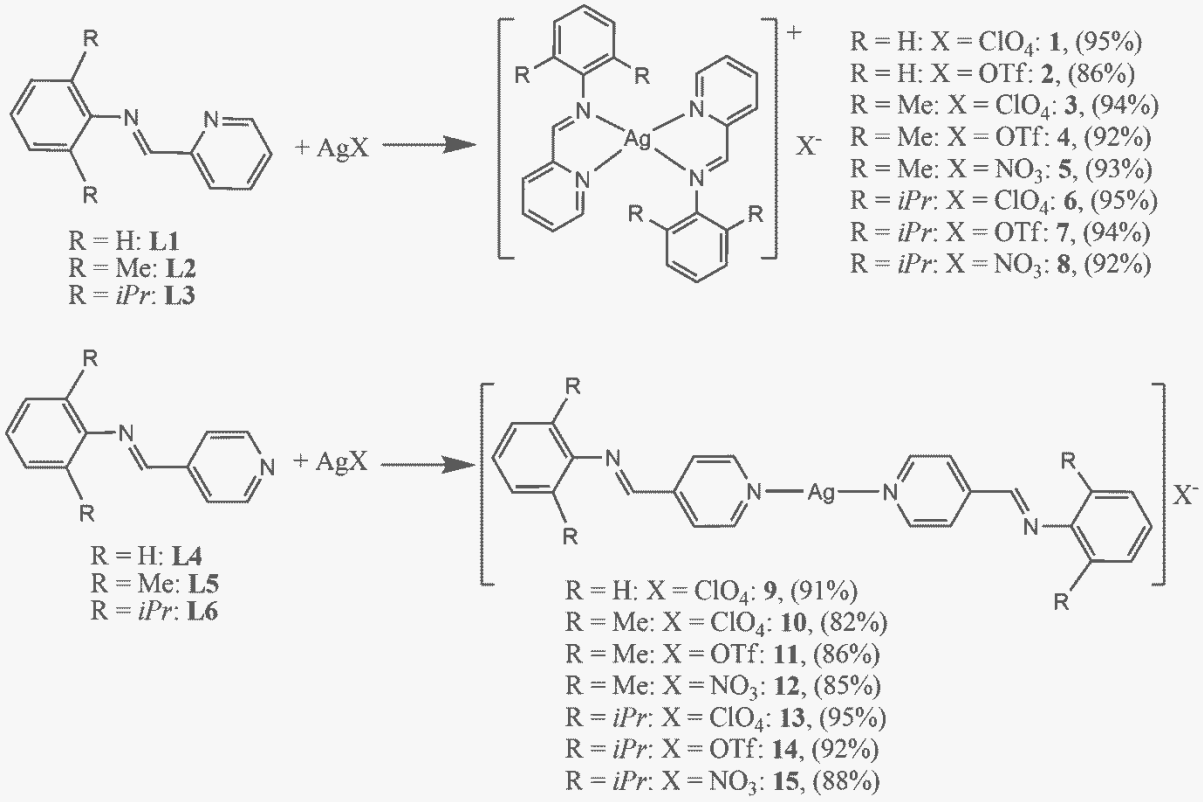

Scheme 2: Synthesis of complexes **1** – **15** *via* magnetic stirring in anhydrous ethanol under inert atmosphere at room temperature. Yield are provided in parentheses.

The NMR studies of the complexes were performed in deuterated d_6-DMSO at room temperature and the results are in agreement with the proposed structures. The resonances associated with pyridinyl and phenyl moieties are unambiguously assigned from their distinctive splitting patterns. For all the complexes reported, only one ligand pattern was observed in the ^{1}H NMR spectra an indication that only one type of complex species was present in solution [78]. The spectra also indicate that in the complex, the ligands coordinating to the metal centres are symmetrical on the NMR timescale. From the ^{1}H NMR spectra of the complexes, there are significant downfield shifts in the resonances of the protons in the vicinity of N atoms involved in the coordination on comparison with free ligands. In complexes **1** – **8**, the azomethine protons and the alpha protons with respect to the N atom in the pyridine rings are shifted downfield when compared to their resonance position in the free ligands. This indicates that the 2-pyrdinyl derivatives, **L1** – **L3** coordinate the silver(I) centres in a chelating mode. This is consistent with other reported complexes of similar ligands [79]. Factors that contribute substantially to the change in chemical shift between the free ligands and the coordinated ligands are the transfer of electrons from the

pyridinyl rings or the imine bonds to the silver(I) ion and polarization effects [80]. These effects are extended to the entire ligand moiety, but the alpha protons are more influenced by coordination than the rest, hence there is a change in the resonance of the alpha protons in going from the free ligands to the complexes. Coordination of silver(I) to the N atoms causes a shift in the electrons from the ligands towards the metal centre, thus the alpha protons are deshielded in the complexes hence resonate further downfield. The downfield shift is consistent with an increase in double bond character of the C–N bond [80]. These shifts point towards coordination of the silver(I) ions by the ligands through both the pyridinyl and the imine N atoms. The shift in resonance of the azomethine protons in ligands **L4** – **L6** is insignificant when compared to the same protons in complexes **9** – **15** an indication that the imine N atoms in these complexes are not involved in the coordination of silver(I) centres [81]. The chemical shifts of significant protons in the complexes are tabulated (Table 3). The spectra of the analogues complexes with perchlorate, nitrate and trifluoromethanesulfonate salts are all very similar, implying they have comparable solution species, that are not affected by the counter anions [82]. The ^{13}C NMR spectra of complexes and free ligands show only slight changes in resonances. The azomethine carbon resonates at 159 – 163 ppm in the complexes.

Table 3: ^{1}H NMR chemical shifts of some protons in the silver(I) complexes **1** – **15** in DMSO-d_6

complex	**1**	**2**	**3**	**4**	**5**	**6**	**7**	**8**	**9**	**10**	**11**	**12**	**13**	**14**	**15**
Ha-Py	8.80	8.80	8.76	8.71	8.69	8.40	8.38	8.52	8.77	8.78	8.78	8.78	8.78	8.78	8.78
CH=N	9.09	9.03	8.63	8.57	8.61	8.59	8.60	8.61	8.71	8.43	8.42	8.43	8.40	8.41	8.42
CH_3	-	-	2.05	2.00	1.97	0.99	0.99	1.03	-	2.07	2.06	2.07	1.11	1.12	1.10
$CH(CH_3)_2$	-	-	-	-	-	2.91	2.85	2.87	-	-	-	-	2.81	2.82	2.81

The formation of the complexes was further confirmed by mass spectrometry. The mass spectra of the complexes show cation molecular peaks of moieties having 1:2 metal to ligand ratio. For instance, mass spectra for complexes **1** and **2** have a molecular cation peaks at *m/z* 471 $[Ag(L1)_2]^+$ (≈100%) and 289 $[AgL1]^+$ (≈30%). Mass spectra for complexes **3** – **5** and **10** – **12** all have molecular cation peaks at *m/z* 527 (~100%) corresponding to $[Ag(L2)_2]^+$ in complexes **3** – **5** and $[Ag(L5)_2]^+$ in complexes **10** – **12**. Complexes **3**, **5**, **10** and **11** also have a peak with *m/z* 317 that correspond to fragment bearing one metal and one ligand i.e. $[AgL]^+$. Complexes **6** – **8** have molecular cation peaks at *m/z* 639 (≈100%) for $[Ag(L3)_2]^+$. Compound **6** and **8** have *m/z* 373 for the fragment bearing one metal and one ligand

molecule. The molecular cation peaks at *m/z* 639 (≈100%) in spectra of complexes **13 – 15** correspond to $[Ag(L_6)]^+$ fragment. The purity and elemental composition of the complexes was confirmed *via* elemental analysis. All experimental data obtained is consistent with the proposed structure. The percentage composition of the elements found is within acceptable limits (deviations <0.4%) in all complexes. The elemental analyses of the complexes are given in Table 4. The structure of complexes **4** and **7** was further established *via* single crystal X-ray diffraction experiments.

Table 4: Physical and chemical data of the silver(I) complexes **1 – 15**

	Chemical formula	Anal. Calcd.			Anal. Found			M.p	ESI-TOF, $[M]^+$	
		C	H	N	C	H	N	(°C)	Calcd.	Found
1	$C_{24}H_{20}AgClN_4O_4$	50.42	3.53	9.80	50.53	3.29	9.80	149 – 150	471.0739	471.0760
2	$C_{25}H_{20}AgF_3N_4O_3S$	48.32	3.24	9.02	48.69	3.24	8.93	136 – 137	471.0739	471.0731
3	$C_{28}H_{28}AgClN_4O_4$	53.56	4.49	8.92	53.46	4.10	8.92	202	527.1365	527.1376
4	$C_{29}H_{28}AgF_3N_4O_3S$	51.41	4.17	8.27	51.67	3.85	8.17	183 - 184	527.1365	527.1360
5	$C_{28}H_{28}AgN_5O_3$	56.96	4.78	11.86	56.96	4.50	11.81	190 – 191	527.1365	527.1375
6	$C_{36}H_{44}AgClN_4O_4$	58.42	5.99	7.57	58.33	5.71	7.78	250 – 251	639.2617	639.2643
7	$C_{37}H_{44}AgF_3N_4O_3S$	56.27	5.62	7.09	56.71	6.03	751	240 – 241	639.2617	639.3106
8	$C_{18}H_{22}AgN_3O_3$	49.56	5.08	9.63	49.26	4.57	9.53	244 - 245	639.2617	639.2624
9	$C_{24}H_{20}AgClN_4O_4$	50.42	3.53	9.80	50.73	3.36	9.69	190	471.0739	471.0760
10	$C_{28}H_{28}AgClN_4O_4$	53.56	4.49	8.92	53.63	4.10	8.86	210	527.1365	527.1680

11	$C_{29}H_{28}AgF_3N_4O_3S$	51.41	4.17	8.27	51.67	3.76	7.88	140 - 142	527.1365	527.1385
12	$C_{28}H_{28}AgN_5O_3$	56.96	4.78	11.86	56.82	4.60	11.77	157	527.1365	527.1365
13	$C_{36}H_{44}AgClN_4O_4$	58.42	5.99	7.57	58.32	5.77	7.12	241	639.2617	639.2623
14	$C_{37}H_{44}AgF_3N_4O_3S$	56.27	5.62	7.09	56.70	5.80	7.27	238	639.2617	639.2640
15	$C_{36}H_{44}AgN_5O_3$	61.54	6.31	9.97	61.92	6.30	9.95	235	639.2617	639.2624

3.3 Crystal structures of complexes 4 and 7

Complexes **4** and **7** are discrete mononuclear cationic complexes with their counter anions out of the coordination sphere. The *ORTEP* diagrams along with the crystallographic numbering scheme for complexes **4** and **7**, are shown in Figure 1. The asymmetric unit of complex **4** consists of two mononuclear complex cations, $[Ag(L2)_2]^+$ and two $CF_3SO_3^-$ anions that are out of the coordination sphere. The two cationic molecules in **4** are not related by symmetry and an overlay of the two give an RMSD of 0.961 Å. In contrast, the asymmetric unit in complex **7** has one cationic complex molecule $[Ag(L3)_2]^+$ and one free $CF_3SO_3^-$ anion. This type of coordination and arrangement in the asymmetric units has been reported for silver(I) complexes with bis(pyridyl) ligands [83, 84]. In both complexes **4** and **7**, two ligand molecules chelate the Ag(I) centres through the pyridine N (N_{py}) and imine N atoms (N_{im}). The coordination generates two five-member rings connected by the Ag(I) centres and having N_{py}—Ag—N_{im} angles averaging at 73.30° (Table 5), in agreement to similar Ag(I) complexes [85]. Each of the five membered ring in the molecules is planar and are orthogonal to each other with dihedral angles of 82.31(5) and 82.44(5)° in the two molecules of complex **4**. The angle is slightly acute, 75.72(3)°, in complex **7** but all three are comparable to those of similar complexes [85]. Besides, the pyridine ring and the metallacycle planes including the imine C atoms form one plane while the phenyl rings including the imine N atoms form another plane. These sets of planes are nonplanar and their dihedral angles in complex **4** are 80.80(7) and 77.59(5)° in one molecule while in the second molecule the angles are 83.98(5) and 78.88(4)°. Similarly, the two sets of planes in the molecule of complex **7** have dihedral angles of 62.76(3) and 86.15(5)°. The noticeable differences between the two molecules in complex **4** suggest that each belong to the C_1 point group and therefore highly unsymmetrical.

The silver(I) centres in the two compounds are tetra-coordinate *via* the N_{py} and N_{im} atoms with a distorted tetrahedral geometry, with the N-Ag-N bond angles ranging from 72.51(4) to 139.07(6)° (Table 5), similar to other reported silver(I) complexes with *N*,*N*-bis(pyridyl) ligands [59]. In the two complexes, the Ag-N_{py} bond lengths range from 2.2527(16) to 2.3758(16) Å and are shorter than the Ag-N_{im} bond distances which range from 2.2560(16) to 2.3738(16) Å (Table 3) but all fall within the expected ranges and are as good as other similar Ag-N bond lengths of related compounds [59].

Table 5: Selected bond lengths and bond angles in complexes **4** and **7**

	4	**7**		**4**	**7**
Bond distances					
Ag—N_{py}	2.2527(16)	2.2777(14)	Ag—N_{im}	2.3646(16)	2.3738(15)
	2.3428(16)	2.2995(14)		2.2699(16)	2.3355(12)
	2.3758(16)			2.2560(16)	
	2.2771(16)			2.3411(16)	
Bond angles					
N_{py}—Ag—N_{py}	139.07(6)	128.30(4)	N_{py}—Ag—N_{im}	73.16(6)	72.91(4)
	135.44(6)			73.41(6)	72.51(4)
N_{im}—Ag—N_{im}	127.28(6)	120.29(4)		73.13(6)	135.25(4)
	130.95(6)			72.74(6	138.67(4)
				132.31(6)	
				120.32(6)	
				133.19(6	
				120.90(6)	

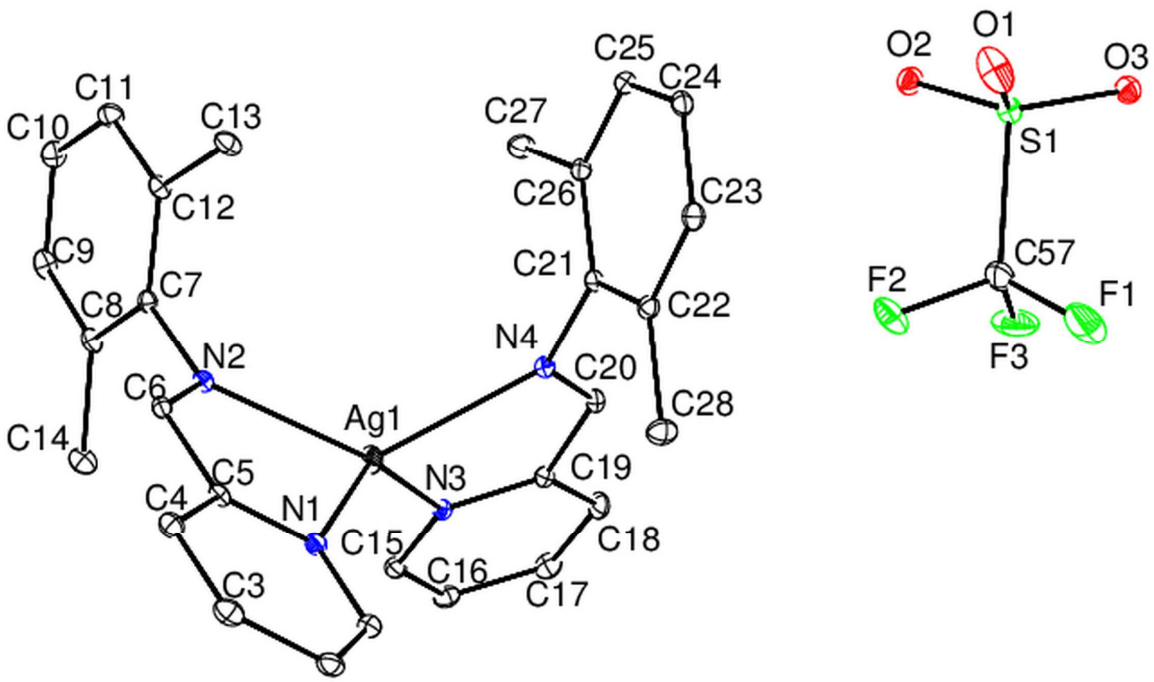
C25
C24
C27
C11
C10
C13
C26
C23
C12
C9
C21
C7
C22
C8
N4
N2
C20
C6
C28
Ag1
C14
C5
N3
C19
C4
N1
C18
C15
C16
C3
C17
O1
O2
O3
S1
C57
F2
F1
F3

(a)

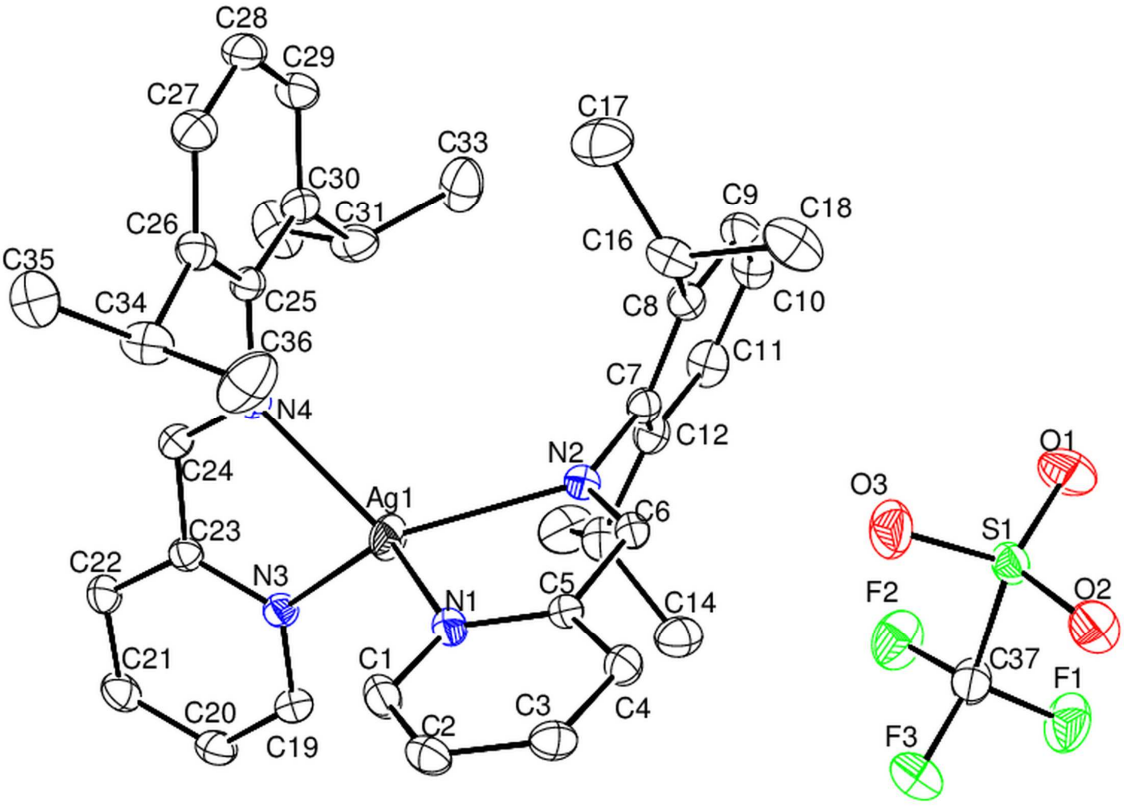
C28
C29
C27
C17
C33
C30
C9
C18
C31
C16
C26
C35
C10
C34
C25
C8
C36
C11
C7
N4
C12
C24
N2
O1
Ag1
O3
C6
C23
S1
C22
N3
C5
C14
N1
F2
O2
C21
C1
C37
C3
C4
F1
C20
C2
F3
C19

(b)

Figure 1: The *ORTEP* diagrams showing the atom numbering scheme with the thermal ellipsoids drawn at the 50% probability level for; (a) one of the two molecules in complex **4** and (b) molecule of complex **7**. Hydrogen atoms have been omitted for clarity.

3.4 *In vitro* anti-bacteria susceptibility tests

The metal-free ligands (**L1** – **L6**) and their silver(I) complexes (**1** – **15**) were screened for their *in vitro* antibacterial activity against gram-negative bacteria *Escherichia coli* and *Salmonella typhimirium*, gram-positive bacterium *Staphylococcus aureus* and the fungus *Candida albicans* using the agar disc diffusion method. Chloramphenicol was used as a standard for the bacteria and fluconazole used as a standard for the fungus. The antimicrobial activities of the compounds **1** – **15** (2 mg mL^{-1}) were obtained from the screening studies are reported in Table 6 as averages of three measurements. Minimum inhibitory concentrations (MIC, μg mL^{-1}) for the compounds against *Escherichia coli* were also determined and are listed in Table 6.

These complexes showed mild activity against gram negative bacterium *Escherichia coli*. The complexes **9** – **6**, that were obtained from 4-pyridinyl ligands (**L4** – **L6**), showed higher activity than complexes **1** – **8** obtained from 2-pyridinyl derivatives. This could be due to the higher stability of cationic complexes **1** – **8**, which reduced the bioavailability of silver(I) ions, hence compromising and plummeting their potency in inhibition of bacterial growth. This stems from the proposition that biological activity of silver(I) complexes is fundamentally dependent on the simplicity of displacing the synthetic ligands from the complexes by ligands in biological systems such as enzymes, proteins, and membranes [37]. The mild activities recorded here indicate that these complexes are highly stable. Consequently, their ligands (that essentially play the role of delivering silver(I) ions to the biological system) could not be easily displaced by biological ligands like proteins and DNA, albeit the presence Ag-N bonds [38, 86, 87]. These complex molecules are also relatively bulky hence it's hard for them to be inserted into DNA helical chains in the bacterial molecules thus unavailable to disrupt the microorganisms biological processes, as a consequence they show lesser inhibition [88].

Surprisingly, the silver(I) complexes were generally ineffective towards inhibiting bacterial growth against the gram positive bacteria used in this study. However, inactivity of silver(I) complexes against these microorganisms is not entirely unusual and has been reported in

other studies [77]. The compounds studied are selective against Gram-negative bacteria as portrayed by their good inhibition against *Escherichia coli*. Silver complexes have been are reported to show relatively higher selectivity against *Escherichia Coli* compared to the Gram-positive bacteria species [89]. This selectivity could have resulted from the structural dissimilarities between Gram-positive and negative bacterial cells, though the precise causes for the discrepancy are not yet clear. Also, *Salmonella typhimirium* could have shown resistance to the complexes studied here, as has been reported in other silver(I) complexes [15, 90, 91].

Table 6: Antimicrobial activity of the complexes **1 - 15**

	Diameter of inhibition zone, Ø (mm)				MIC (μgmL^{-1})
complex ($2mgmL^{-1}$)	*Escherichia coli*	*Salmonella typhimirium*	*Staphylococcus aureus*	*Candida albicans*	*Escherichia Coli*
1	11	-ve	-ve	+ve	120
2	11	-ve	-ve	-ve	125
3	11	-ve	-ve	-ve	140
4	10	-ve	-ve	-ve	130
5	10	-ve	-ve	-ve	130
6	7	-ve	-ve	-ve	200
7	7	-ve	-ve	-ve	180
8	11	-ve	-ve	-ve	120
9	12	-ve	-ve	8	80
10	12	-ve	-ve	+ve	100
11	13	-ve	-ve	+ve	80
12	14	-ve	-ve	+ve	80
13	11	-ve	-ve	+ve	130
14	8	-ve	-ve	+ve	120
15	13	-ve	-ve	+ve	100
DMSO	0	0	0	0	0
Chloramphenicol	20	23	20	Not tested	30
Fluconazole	Not tested	Not tested	Not tested	22	Not tested

Key: '-ve' no activity; '+ve' low activity with an inhibition zone of diameter 6 mm

Conclusion

The work reported herein demonstrates how pyridinyl Schiff base ligands can be synthesised effortlessly *via* mechanochemistry techniques. The reactions were achieved within record time and the target (*E*)-*N*-(pyridinylmethylene)aniline ligands (**L1** - **L6**) obtained in excellent yields. The (*E*)-*N*-(pyridinylmethylene)aniline ligands **L1 – L6** were successfully employed in synthesis of fifteen new structure-related silver(I)-pyridinyl complexes. The complexes were successfully characterised using NMR and FTIR spectroscopies, mass spectrometry, melting points, microanalysis and some by single crystal X ray diffraction technique. The proposed molecular structures are unambiguous and perfectly agree with the analytical data obtained. The 2-pyridinyl derivatives ligands **L1** – **L3** yielded complexes in which the silver(I) ions were chelated *via* the pyridinyl and imine N donors. On the other hand, the 4-pyridinyl ligands **L4** – **L6** coordinated only using the pyridinyl N atoms. Structure of complexes **4** and **7** of silver trifluoromethanesulfonate with pyridin-2-ylmethyleneaniline derivatives **L2** and **L3**, respectively were determined by single crystal X-ray diffraction technique. The structural motifs obtained show the complexes are mononuclear and cationic with well separated anions. This coordination pattern corresponds to known modes of this type of ligand towards silver(I), in which the ligands chelate the metal centres *via* the pyridinyl and imine N atoms. The complexes showed moderate antibacterial activity against bacterium *Escherichia Coli*, but were inactive against bacteria *Staphylococcus aureus* and *Salmonella typhimirium*. The activities of the silver(I)-pyridinyl Schiff base complexes reported here are attributable to ligand substitution with the biological ligands such as proteins and DNA. The moderate activities portray high stability of the complexes especially the chelates. Thus, their ligands were thus difficult to dislodge by the biological ligands and silver(I) ions were not readily bioavailable. The complexes showed high selectivity against gram *Escherichia coli*. The antimicrobial results underpin the need to balance between ambience and photo stability of silver(I) complexes against their dissolution and transport in biological systems. Synthesis of enzyme targeted ligands and their silver(I) complexes as well as structure activity relationships is desired to further understand the bioactivity and resistance portrayed.

Supplementary data

CCDC 1498656 and 1498657 contains the supplementary crystallographic data for compounds **4** and **7** respectively. This data is available free of charge from the CCDC.

Acknowledgement

The authors acknowledge the financial support by University of KwaZulu-Natal and National Research Foundation (South Africa). We are grateful to Mr Sizwe Joshua Zamisa for his vital assistance in single X-ray experiments.

REFERENCES

[1] J. Davies, D. Davies, Microbiology and Molecular Biology Reviews, 74 (2010) 417-433.

[2] A.J. Alanis, Archives of Medical Research, 36 (2005) 697-705.

[3] G. McDonnell, A.D. Russell, Clinical Microbiology Reviews, 12 (1999) 147-179.

[4] B.A. Cunha, Medical Clinics of North America, 85 (2001) 149-185.

[5] I. Chopra, Journal of Antimicrobial Chemotherapy, 59 (2007) 587-590.

[6] H. Klasen, Burns, 26 (2000) 131-138.

[7] M.J. Carter, K. Tingley-Kelley, R.A. Warriner, Journal of the American Academy of Dermatology, 63 (2010) 668-679.

[8] J. Fong, international Journal of Nanomedicine, 1 (2006) 441-449.

[9] A. Kascatan-Nebioglu, M.J. Panzner, C.A. Tessier, C.L. Cannon, W.J. Youngs, Coordination Chemistry Reviews, 251 (2007) 884-895.

[10] P.J. Stanirowski, A. Wnuk, K. Cendrowski, W. Sawicki, Archives of gynecology and obstetrics, 292 (2015) 757-775.

[11] I. Sondi, B. Salopek-Sondi, Journal of Colloid and Interface Science, 275 (2004) 177-182.

[12] J.S. Kim, E. Kuk, K.N. Yu, J.-H. Kim, S.J. Park, H.J. Lee, S.H. Kim, Y.K. Park, Y.H. Park, C.-Y. Hwang, Nanomedicine: Nanotechnology, Biology and Medicine, 3 (2007) 95-101.

[13] C. Banti, A. Giannoulis, N. Kourkoumelis, A. Owczarzak, M. Poyraz, M. Kubicki, K. Charalabopoulos, S. Hadjikakou, Metallomics, 4 (2012) 545-560.

[14] R.L. Davies, S.F. Etris, Catalysis Today, 36 (1997) 107-114.

[15] S. Percival, P. Bowler, D. Russell, Journal of Hospital Infection, 60 (2005) 1-7.

[16] S. Rajeshkumar, C. Malarkodi, M. Vanaja, G. Annadurai, Journal of Molecular Structure, (2016).

[17] S. Glišić, M. Cakić, G. Nikolić, B. Danilović, Journal of Molecular Structure, 1084 (2015) 345-351.

[18] U. Kalinowska-Lis, A. Felczak, L. Chęcińska, I. Szabłowska-Gadomska, E. Patyna, M. Małecki, K. Lisowska, J. Ochocki, Molecules, 21 (2016) 87.

[19] S. Ahmad, A.A. Isab, S. Ali, A.R. Al-Arfaj, Polyhedron, 25 (2006) 1633-1645.

[20] J. Schierholz, L. Lucas, A. Rump, G. Pulverer, Journal of Hospital Infection, 40 (1998) 257-262.

[21] A. Kantouch, A.A. El-Sayed, International Journal of Biological Macromolecules, 43 (2008) 451-455.

[22] Y. Barnea, J. Weiss, E. Gur, Therapeutics and Clinical Risk Management, 6 (2010) 21.

[23] Z. Aziz, S. Abu, N. Chong, Burns, 38 (2012) 307-318.

[24] C.L. Fox, Archives of Surgery, 96 (1968) 184-188.

[25] M.C. Fung, D.L. Bowen, Clinical Toxicology, 34 (1996) 119-126.

[26] B. Thati, A. Noble, B.S. Creaven, M. Walsh, M. McCann, M. Devereux, K. Kavanagh, D.A. Egan, European Journal of Pharmacology, 602 (2009) 203-214.

[27] K.A. Ali, M.M. Abd-Elzaher, K. Mahmoud, International Journal of Medicinal Chemistry, 2013 (2013).

[28] C.N. Banti, S.K. Hadjikakou, Metallomics, 5 (2013) 569-596.

[29] B.K. Banik, F.F. Becker, European Journal Of Medicinal Chemistry, 45 (2010) 4687-4691.

[30] M.S. Mohamed, Y.E.E.-D. Awad, S.M. El-Hallouty, M. El-Araby, Open Journal of Medicinal Chemistry, 2 (2012), 78-88.

[31] M. Baia, L. Baia, W. Kiefer, J. Popp, The Journal of Physical Chemistry B, 108 (2004) 17491-17496.

[32] C.-H. Kuo, C.-Y. Lu, Y.-C. Yang, C. Chin, B.-C. Weng, C.-J. Liu, Y.-H. Chen, L.-L. Chang, F.-C. Kuo, D.-C. Wu, BioMed Research International, 2014 (2014).

[33] S. Günal, N. Kaloğlu, İ. Özdemir, S. Demir, İ. Özdemir, Inorganic Chemistry Communications, 21 (2012) 142-146.

[34] A. Panáček, L. Kvitek, R. Prucek, M. Kolar, R. Vecerova, N. Pizurova, V.K. Sharma, T.j. Nevečná, R. Zboril, The Journal of Physical Chemistry B, 110 (2006) 16248-16253.

[35] B. Thati, A. Noble, R. Rowan, B.S. Creaven, M. Walsh, M. McCann, D. Egan, K. Kavanagh, Toxicology *in vitro*, 21 (2007) 801-808.

[36] B.S. Creaven, D.A. Egan, K. Kavanagh, M. McCann, M. Mahon, A. Noble, B. Thati, M. Walsh, Polyhedron, 24 (2005) 949-957.

[37] I. Tsyba, B.B.-k. Mui, R. Bau, R. Noguchi, K. Nomiya, Inorganic Chemistry, 42 (2003) 8028-8032.

[38] K. Nomiya, K. Tsuda, T. Sudoh, M. Oda, Journal of Inorganic Biochemistry, 68 (1997) 39-44.

[39] G. Malicorne, J. Bompart, L. Giral, E. Despaux, European Journal of Medicinal Chemistry, 26 (1991) 3-11.

[40] C. Bouillon, G. Kalopissis, G. Lang, in, Google Patents, 1975.

[41] I. Ostromislensky, in, Google Patents, 1928.

[42] S.L. Hargreaves, B.L. Pilkington, S.E. Russell, P.A. Worthington, Tetrahedron Letters, 41 (2000) 1653-1656.

[43] N. Aggarwal, R. Kumar, P. Dureja, D.S. Rawat, Journal of Agricultural and Food Chemistry, 57 (2009) 8520-8525.

[44] U. Singh, S. Pandeya, A. Singh, B. Srivastava, M. Pandey, International Journal Pharmaceutical Science Drug Research, 2 (2010) 151-154.

[45] Z.-M. Lian, J. Sun, H.-L. Zhu, Journal of Molecular Structure, 1117 (2016) 8- 6.

[46] O. Kayser, A. Kiderlen, S. Croft, Parasitology Research, 90 (2003) S55-S62.

[47] B.S. Creaven, B. Duff, D.A. Egan, K. Kavanagh, G. Rosair, V.R. Thangella, M. Walsh, Inorganica Chimica Acta, 363 (2010) 4048-4058.

[48] A. Chakraborty, P. Kumar, K. Ghosh, P. Roy, European Journal of Pharmacology, 647 (2010) 1-12.

[49] M.S. Alam, J.-H. Choi, D.-U. Lee, Bioorganic & Medicinal Chemistry, 20 (2012) 4103-4108.

[50] D. Sriram, P. Yogeeswari, N.S. Myneedu, V. Saraswat, Bioorganic & Medicinal Chemistry Letters, 16 (2006) 2127-2129.

[51] C.M. da Silva, D.L. da Silva, L.V. Modolo, R.B. Alves, M.A. de Resende, C.V. Martins, Â. de Fátima, Journal of Advanced Research, 2 (2011) 1-8.

[52] R. Sahu, D. Thakur, P. Kashyap, International Journal of Pharmaceutical Sciences and Nanotechnology, 5 (2012) 1757-1764.

[53] P. Anand, V. Patil, V. Sharma, R. Khosa, N. Masand, International Journal of Drug Design and Discovery, 3 (2012) 851-868.

[54] G. Dong, H. Cheng, D. Chun-Ying, Q. Chun-Qi, M. Qing-Jin, New Journal of Chemistry, 26 (2002) 796-802.

[55] D.-B. Dang, G.-S. Zheng, Y. Bai, Journal of Inorganic and Organometallic Polymers and Materials, 20 (2010) 356-360.

[56] W.-J. Niu, J.-L. Wang, Y. Bai, D.-B. Dang, Spectrochimica Acta Part A: Molecular and Biomolecular Spectroscopy, 91 (2012) 61-66.

[57] L.Y. Jin, M.M. Li, D.B. Dang, Y. Bai, Y.N. Zheng, Zeitschrift für Naturforschung B, 68 (2013) 284-288.

[58] J. Hamblin, A. Jackson, N.W. Alcock, M.J. Hannon, Journal of the Chemical Society, Dalton Transactions, (2002) 1635-1641.

[59] F. Tuna, J. Hamblin, G. Clarkson, W. Errington, N.W. Alcock, M.J. Hannon, Chemistry–A European Journal, 8 (2002) 4957-4964.

[60] G.K. Patra, I. Goldberg, Crystal Growth & Design, 3 (2003) 321-329.

[61] D. Dang, G. Zheng, Y. Bai, F. Yang, H. Gao, P. Ma, J. Niu, Inorganic chemistry, 50 (2011) 7907-7909.

[62] F. Chen-jie, D. Chun-ying, M. Hong, H. Cheng, M. Qing-jin, L. Yong-jiang, M. Yu-hua, W. Zhe-ming, Organometallics, 20 (2001) 2525-2532.

[63] T.V. Laine, U. Piironen, K. Lappalainen, M. Klinga, E. Aitola, M. Leskelä, Journal of Organometallic Chemistry, 606 (2000) 112-124.

[64] R. Montalvo-González, A. Ariza-Castolo, Journal of Molecular Structure, 655 (2003) 375-389.

[65] L. Troisi, L. Ronzini, C. Granito, L. De Vitis, E. Pindinelli, Tetrahedron, 62 (2006) 1564-1574.

[66] A. Köppl, H.G. Alt, Journal of Molecular Catalysis A: Chemical, 154 (2000) 45-53.

[67] A. Mechria, S. Dridi, M. Msaddek, Inorganica Chimica Acta, 427 (2015) 173-177.

[68] A.V. Bruker, Inc., Madison, WI, USA, (2009).

[69] G. Sheldrick, University of Göttingen: Germany, (2013).

[70] L.J. Farrugia, Applied Crystallography, 45 (2012) 849-854.

[71] A.D. Khalaji, K. Aoki, M. Amirnasr, Journal of Coordination Chemistry, 60 (2007) 201-206.

[72] F. Farha Jr, R.T. Iwamoto, Inorganic Chemistry, 4 (1965) 844-848.

[73] Y. Chen, Y.-H. Zhang, L.-J. Zhao, Physical Chemistry Chemical Physics, 6 (2004) 537-542.

[74] P.J. Riedel, N. Arulsamy, M.P. Mehn, Inorganic Chemistry Communications, 14 (2011) 734-737.

[75] Z.-F. Chen, Y.-Z. Tang, H. Liang, H.-K. Fun, K.-B. Yu, Journal of Coordination Chemistry, 59 (2006) 207-214.

[76] L. Cheng, L. Zhang, S. Gou, Q. Cao, J. Wang, L. Fang, CrystEngComm, 14 (2012) 3888-3893.

[77] S. Nawaz, A.A. Isab, K. Merz, V. Vasylyeva, N. Metzler-Nolte, M. Saleem, S. Ahmad, Polyhedron, 30 (2011) 1502-1506.

[78] G.C. Van Stein, G. Van Koten, B. De Bok, L. C. Taylor, K. Vrieze, C. Brevard, Inorganica Chimica Acta, 89 (1984) 29-39.

[79] S.E. Bodman, A.C. Crowther, P.B. Geraghty, C.M. Fitchett, CrystEngComm, 17 (2015) 81-89.

[80] S. Ahmad, A.A. Isab, W. Ashraf, Inorganic Chemistry Communications, 5 (2002) 816-819.

[81] M. Wenzel, K. Wichmann, K. Gloe, K. Gloe, H.-J. Buschmann, K. Otho, M. Schröder, A.J. Blake, C. Wilson, A.M. Mills, CrystEngComm, 12 (2010) 4176-4183.

[82] F. Tuna, G. Clarkson, N.W. Alcock, M.J. Hannon, Dalton Transactions, (2003) 2149-2155.

[83] J. Huang, Z.-P. Deng, Y.-H. Xiao, L.-H. Huo, S.-N. Zhao, F.-Y. Ge, S. Gao, Dalton Transactions, 44 (2015) 5837-5847.

[84] P. Halder, E. Zangrando, T.K. Paine, Dalton Transactions, (2009) 5386-5394.

[85] B. Chakraborty, S. Maiti, T.K. Paine, Polyhedron, 52 (2013) 122-127.

[86] K. Nomiya, S. Takahashi, R. Noguchi, S. Nemoto, T. Takayama, M. Oda, Inorganic Chemistry, 39 (2000) 3301-3311.

[87] A.A. Isab, S. Nawaz, M. Saleem, M. Altaf, M. Monim-ul-Mehboob, S. Ahmad, H.S. Evans, Polyhedron, 29 (2010) 1251-1256.

[88] J.-A. Zhang, M. Pan, J.-Y. Zhang, H.-K. Zhang, Z.-J. Fan, B.-S. Kang, C.-Y. Su, Polyhedron, 28 (2009) 145-149.

[89] X.-Z. Zou, J.-A. Zhang, L.-J. Zhang, Y.-J. Liu, N. Li, Y. Li, S.-C. Wei, M. Pan, Inorganic Chemistry Communications, 54 (2015) 21-24.

[90] G.L. Mchugh, R. Moellering, C. Hopkins, M. Swartz, The Lancet, 305 (1975) 235-240.

[91] S. Silver, FEMS Microbiology Reviews, 27 (2003) 341-353.

Silver(I)-pyridinyl Schiff base complexes: Synthesis, characterization and antimicrobial studies

Eric M. Njogu, Bernard Omondi and Vincent O. Nyamori

School of Chemistry and Physics, University of KwaZulu-Natal, South Africa

Private bag X54001, Durban, 4000

Email: bjumberic2002@gmail.com; owaga@ukzn.ac.za; nyamori@ukzn.ac.za

Highlights

- Silver(I) complexes synthesised by use of (*E*)-*N*-(pyridinylmethylene)aniline ligands
- The compounds were characterised via spectroscopic and X-ray diffraction techniques
- The complexes were investigated for antimicrobial activity